Food Chemistry 115 (2009) 1491–1499

Contents lists available at ScienceDirect

Food Chemistry

journal homepage: www.elsevier.com/locate/foodchem

The effect of rice kernel microstructure on cooking behaviour: A combined μ-CT and MRI study

Aleš Mohorič [a,*,1], Frank Vergeldt [a], Edo Gerkema [a], Gerard van Dalen [b], L.R. van den Doel [c,2], L.J. van Vliet [c], Henk Van As [a], John van Duynhoven [b]

[a] Laboratory of Biophysics and Wageningen NMR Centre, Wageningen University, Dreijenlaan 3, 6703 HA Wageningen, The Netherlands
[b] Unilever R&D, Vlaardingen, Olivier van Noortlaan, P.O. Box 114, 3130 AC Vlaardingen, The Netherlands
[c] Quantitative Imaging Group, Delft University of Technology, Lorentzweg 1, NL-2628 CJ Delft, The Netherlands

ARTICLE INFO

Article history:
Received 31 October 2008
Received in revised form 15 December 2008
Accepted 27 January 2009

Keywords:
MRI
XRT
μCT
Microtomography
Modelling
Rice
Cooking
Microstructure

ABSTRACT

In order to establish the underlying structure-dependent principles of instant cooking rice, a detailed investigation was carried out on rice kernels that were processed in eight different manners. Milling, parboiling, wet-processing and extrusion were applied, with and without a subsequent puffing treatment. The mesostructure of the rice kernels was examined by DSC and XRD, and the microstructure by μ-CT. Hydration behaviour during cooking was studied by MRI in a real-time manner. Based on simple descriptive models, three different classes of cooking behaviour can be discerned. The water ingress profiles during cooking of these three classes matched well with simulations from a model that was based on water demand of the starch mass and the porous microstructure of the kernels. Thus a clear correlation between meso/microstructure of a rice kernel and the cooking behaviour has been established.

1. Introduction

Rice is a staple food that provides more than half of the world's population with carbohydrates in the form of starch. In rice kernels, starch is stored in granules, i.e. concentric layers of molecular oriented, branched amylopectin in which molecular stacked, crystalline amylose is packed. Cooking rice involves wetting of the kernels up to a moisture content of 65–70%. This wetting process results in swelling of the kernel. Whilst the melting of the amylopectin crystals takes place, release of amylose from the starch granules, and gel formation takes place. In this way, rice becomes a soft, easily masticateable product, ready for consumption. Industrial processes are known to enhance the texture and nutritional value of cooked rice, or add extra convenience like instant preparation. Parboiling (Bhattacharya, 1985) is a traditional process, which involves heating of rice kernels in their hull (paddy), at relatively low moisture. In this way, part of the nutrients originally present in the germ, are driven into the kernel, making the nutritional value of parboiled rice higher than that of white rice. After the parboiling process, the rice is dehusked (removal of indigestible fibre material) and polished (removal of digestible bran and in most cases also the germ). For white rice, dehusking and milling is done after the conditioning and drying of the paddy without the application of any heating process. Due to the low moisture content and the limited space of the kernel in the husk, the kernel can hardly swell during the parboiling process. Therefore, after drying and further processing, the parboiled rice kernel is more compact than the untreated (white) rice kernel, resulting in longer cooking times. The mechanical properties and texture have changed and the colour has become slightly yellowish.

To increase convenience for consumers, the food industry has engineered other pre-treatment processes to obtain, for example, shorter preparation times. During wet-processing (Lee, Lim, Jae-Kag, & Seung-Taik, 2000) polished rice is cooked and subsequently dried, which is very effective in reducing the cooking time at the

Abbreviations: E, extruded; EP, extruded and puffed; M, milled; MP, milled and puffed; NMR, nuclear magnetic resonance; MRI, magnetic resonance imaging; P, parboiled; PDE, partial differential equations; PP, parboiled and puffed; XRT, X-ray tomography; μ-CT, micro computer tomography; W, wet-processed; WD, water demand; WP, wet-processed and puffed.

* Corresponding author. Tel.: +386 1 4766552; fax: +386 1 2517281.
E-mail address: ales.mohoric@fmf.uni-lj.si (A. Mohorič).
[1] Present address: Faculty of Mathematics and Physics, University of Ljubljana, Jadranska 19, 1000 Ljubljana, Slovenia.
[2] Present address: Roosevelt Academy, Lange Noordstraat 1, NL-4331 CB, Middelburg, The Netherlands.

0308-8146/$ - see front matter © 2009 Elsevier Ltd. All rights reserved.
doi:10.1016/j.foodchem.2009.01.089

expense of texture. Extrusion of rice flour (Gonzalez, Torres, De Greef, & Guadalupe, 2006; Guha, 2006) into gelatinised, reformed kernels results in a product with a similar poor compromise between cooking time and texture. Puffing (Murugesan & Bhattacharya, 1986) involves heating of rice kernels at high temperature and low moisture conditions. Puffing raw rice results in a product which still requires cooking, but the cooking time is reduced and the final product properties are relatively good. Gelatinising the starch in the kernels before puffing gives a higher expansion ratio, resulting in a further reduction of the preparation time (instant preparation or cooking). Depending on the applied processing steps and equipment, the eating properties of highly puffed rice kernels can vary from grittiness, lacking cohesion and bite, up to acceptable eating properties.

The impact of these processing steps on consumer relevant properties of rice (Blakeney, 1996; van Dalen, 2006) such as texture and appearance has been studied extensively. Currently, we know that the structural features that determine rice cooking are the limited rate of water uptake due to material compactness, the presence of crystalline starch and starch complexes, compactness of glassy starch structures, and kernel micro-porosity (Horigane et al., 2000; Lai & Cheng, 2004). An understanding of these properties at the molecular, mesoscopic and microstructural level is typically based on studies where the impact of one process on one or few structural features is investigated (Chandrasekhar & Chattopadhyay, 1990; Ruan et al., 1997).

In this study we used μ-CT, MRI, DSC, XRD, and descriptive as well as structure-based modelling to investigate the impact of combinations of different processing steps on the molecular-, meso- and microstructure of rice kernels in relation to their macroscopic properties. We first subjected rice kernels of a widely grown rice variety, IR64, to either parboiling, wet-processing or extrusion in order to change their molecular and mesoscopic order. Subsequently, these processed kernels were subjected to a puffing step in order to introduce a more porous (from sponge to honey comb) structure. From previous work (Ramesh, Bhattacharya, & Mitchel, 2000) we can expect that parboiling, wet-processing and extrusion will result in melting of the A-type amylose and that after cooling amorphous amylose will convert into retrograded B- and V-type polymorphs. One can also expect that the subsequent puffing step will result in relatively modest additional (re)gelatinisation of starch.

In our current study, we departed from the hypothesis that heating rice under appropriate conditions, such as the presence of water and certain temperatures, results in gelatinisation of the starch and the formation of a homogeneous starch/protein mass surrounded by the originally present and still intact plant cell walls in the kernel. Expansion of the kernel results from the formation of air-cells in this rice material. Air-cells form after the water evaporates to steam, thereby requiring more volume (Mariotti, Alamprese, Pagani, & Lucisano, 2006). The events that occur at the molecular and mesoscopic level were assessed by differential scanning calorimetry (DSC) and X-ray diffraction (XRD). The impact of the different processing steps on the kernel's microstructure and hydration behaviour was investigated by joint deployment of X-ray microtomography (μ-CT) and magnetic resonance imaging (MRI). μ-CT is superior for assessment of 3D porous microstructures under low moisture conditions (van Dalen, Nootenboom, van Vliet, Voortman, & Esveld, 2007), whereas MRI can monitor the relation between microstructure and water ingress during cooking in a real-time manner (Kasai, Lewis, Ayabe, Hatae, & Fyfe, 2007; Kasai et al., 2005; Mohorič et al., 2004). The combination of μ-CT and dynamic MRI experiments opens up the possibility to establish relations between the meso- and microstructure of rice kernels on one hand, and their cooking behaviour, in particular moisture transport during cooking, on the other hand. Models for moisture transport during cooking of starchy foods, however, often do not obey existing conventional mass transport models. These models are generally based on an assumption that diffusion of moisture is driven by differences in water content, i.e. Fickian diffusion. However, the changes in moisture content are much slower than can be expected from simple Fickian diffusion (Stapley, Hyde, Gladden, & Fryer, 1997; Takeuchi, Fukuoka, Gomi, Maeda, & Watanabe, 1997; Takeuchi, Maeda, Gomi, Fukuoka, & Watanabe, 1997; Watanabe, Fukuoka, Tomiya, & Mihori, 2001). Attempts have been made to describe such behaviour by Case II Fickian diffusion models but in recent work much better predictions were obtained by introducing the concept that water migration is driven by water demand (WD), defined as the difference between the maximum moisture content, and the existing one (Fukuoka, Mihori, & Watanabe, 2000; Watanabe et al., 2001). In other words, WD is the amount of water the starch can potentially accept. It has been shown that the WD model can predict moisture profiles in water–starch model systems as well as in untreated, homogeneous, rice kernels (Watanabe et al., 2001). The impact of WD in conjunction with structural heterogeneities in the kernel (e.g. pores and cracks), has not been established yet. Thus we also deployed a structure-based model (van den Doel et al., in press) that comprised WD functions and the microstructure of the kernel as determined by μ-CT. The purpose of this model was to assess the hypothesised impact of these structural features on the cooking behaviour of (processed) rice kernels.

2. Materials and methods

2.1. Materials

Rice kernels of the Indonesian IR 64 rice were used as the starting material for further processing using milling (M), parboiling (P), wet-processing (W) and extrusion (E). Also a series was prepared where these kernels were subsequently puffed (MP, PP, WP and EP, respectively). Details of processing conditions are described below. Samples were kept at room temperature in closed bags until use. The plain milled IR 64 rice kernels contain 80% starch, 10% protein, 0.3% fat and 10% water.

2.2. Methods

2.2.1. Rice processing

2.2.1.1. Parboiled rice (P). Paddy rice (in the husk) was soaked in water at 60 °C, until the moisture content of the kernels was 30–35%. After this, the paddy was steamed, either for 60–80 min at atmospheric pressure or about 15 min at 1 bar overpressure. The aim of this heating step was to obtain fully gelatinised starch. The rice (still in the husk) was dried at either ambient or increased temperatures (max. 60 °C) until the moisture content was 16–18%. The rice was dehusked and milled (bran is removed), and further conditioned to a moisture content of about 10–12%.

2.2.1.2. Wet-processed rice (W). White rice (raw rice, without husk and bran) was soaked at 70 °C to a moisture content of about 30%. The kernels were steamed at atmospheric pressure (approx. 100 °C) to get full gelatinisation of the starch and this was subsequently dried at ambient conditions.

2.2.1.3. Extrusion. White rice (same material as used in the wet-processing) was ground to flour. The flour was fed into a cooking extruder after it was heated (to about 90 °C) and moisturised in a pre-conditioner. The extrusion process took place at high pressure (30 to 40 bar at the end of the barrel) and increased temperature (barrel temperature of approx. 90 °C). After extrusion, the

reconstituted kernels were dried at around 60 °C, from 35% down to 12% moisture content.

2.2.1.4. Puffed rice (MP, PP, WP, EP). Milled rice (M) and the various processed rice samples (P, W, E) were further treated in a high temperature environment to obtain puffed kernels. A hot (280–300 °C) dry air stream was used to bring kernels into a fluidised bed. The treatment was relatively short, about 14 s, and resulted in expansion of the kernels. This process was performed in batch mode, using scale equipment in a pilot plant. Hereafter, the kernels were cooled to room temperature, packed and stored at ambient temperatures.

2.2.2. X-ray microtomography (μ-CT)

The internal porous structure of the rice kernels was visualised using a SkyScan 1072 desktop X-ray microtomography (μ-CT) system (SkyScan, Belgium, http://www.skyscan.be). A power setting of 50 kV and 100 μA was used. Rice kernels were fixed on a specimen holder using glue. A stack of flat cross-sections was obtained after tomographic reconstruction of projection images (1024 × 1024 pixels) acquired under different rotations over 180° with a step size of 0.45°. The actual 3D structure was visualised using 3D surface rendering techniques (Amira 4.1, Mercury Computer Systems, Bordeaux, France). The acquisition time for one projection image was 2.8 s resulting in a total acquisition and read-out time of about 60 min (700 projection images). A magnification factor of 30 was selected, resulting in a pixel size of 9.1 μm. For image processing and analysis the image analysis toolbox (DIPlib version 1.5.0 from the Delft University of Technology, NL, http://www.DIPlib.org) running under MATlab (version 7.1, R14, SP3 from MathWorks) was used.

2.2.3. Magnetic resonance imaging (MRI)

The MRI experiments were conducted on a 0.7 T Bruker Avance MRI system as described elsewhere (Mohorič et al., 2004). Kernels were held in position by glass wool inside a 5 mm o.d. glass tube and an ample amount of water was added. The preparation of a sample took about 5 min. During this time, some cold hydration of the surface layer of kernels may take place. The tube was heated by hot air. The heater was turned on after the first scan was completed at room temperature. Every 75 s an image was acquired during the first 30 min of the cooking process. Each image took 64 s of scan time. The temperature in the tube reached the cooking temperature (at 90 °C well above the gelatinisation temperature of 81 °C) within a minute of the heater being turned on and was kept constant to within a few degrees during the cooking period. The stability of the temperature was sufficient to neglect the relative change in gelatinisation rate as a function of temperature (Gomi, Fukuoka, Mihori, & Watanabe, 1998). A centered out 3D RARE imaging sequence (Scheenen, van Dusschoten, de Jager, & Van As, 2000) was used to record images with a 128 × 32 × 16 matrix and a voxel volume of 117 × 156 × 313 μm^3. The experiment was performed with TR = 500 ms and TE = 6.6 ms.

2.2.4. Differential scanning calorimetry (DSC)

Thermograms were recorded using a Perkin–Elmer power compensated Pyris-1 equipped with a controlled cooling accessory using liquid nitrogen as the cooling agent. Rice kernels were first ground in a Retsch mill using a 0.2 mm sieve. Approximately 15 mg of ground powder was accurately weighed into the sample pan and two drops of tap water were added. Measurements were started 3 h after the first weighing was completed.

2.2.5. X-ray diffraction (XRD)

Diffraction lines of the samples were obtained with a Bruker-Nonius D8 Discover diffractometer. The instrument was equipped with a water-cooled rotating copper anode that produces Cu Kα X-rays with an accelerating voltage 40 kV and a tube current 40 mA. An angular range (2θ) was scanned between 4° and 25°. The detection limit of XRD was ±3% depending on the intensity of the peaks found. From the diffraction pattern the crystalline compounds were identified. The crystallinity of each sample was calculated from the relative area of peaks to the whole region over the background line.

2.2.6. Gravimetric assessment of water uptake during cooking

The total weight of 10 rice kernels was determined in dry status and after they had been immersed in water (at room temperature or boiling) for increasing periods of time. The wet kernels were blotted with paper tissue before weighing.

2.2.7. Quantification of MRI data

The analysis of moisture profiles is based on the NMR signal which corresponds to normalised relative moisture content m (defined as water mass–dry mass ratio), with the baseline subtracted (Mohorič et al., 2004). The baseline moisture content is the lowest moisture content that can be observed in the NMR signal (around 20% in our case). The pixel signal in RARE imaging (Scheenen et al., 2000) is roughly given by:

$$A = A_0[1 - \exp(-\mathrm{TR}/T_1)]\exp(-\mathrm{TE}/T_2), \quad (1)$$

where TR is the imaging sequence repetition time, TE the effective spin echo time of the RARE sequence and A_0 is proportional to local m (number of protons in a pixel) and sensitivity of the imaging apparatus. The variation of longitudinal (spin–lattice) relaxation time T_1 over the sample is small and can be neglected in further analysis (Mohorič et al., 2004). However, the signal is more affected by transversal (spin–spin) relaxation time T_2, which depends on m and temperature – the linear approximation of this dependence is in our case $T_2/\mathrm{ms} = 12m + 2$. Stronger deviation from this linear behaviour is apparent only at low moisture content and hence care should be taken in transforming weak NMR signals to m. The NMR signal from the moisture front thus underestimates m because the signal is weaker, not only because spin density is smaller, but also because the relaxation time is shorter.

For quantitative assessment of the kinetic events occurring during cooking of the rice kernels, two formats are used for data presentation. In one format, a representative 1D plot across the kernel is used. An average signal of 10 surrounding voxels in the direction perpendicular to the 1D profile direction is plotted on the axis that runs through the centre of the kernel and lays in the sagittal plane of the kernel. Spatial inhomogeneities prevent averaging over a larger volume and the different resolution in the coronal plane prevents averaging over the complete 2D axial plane. Alternatively, the 1D signal is integrated, thus providing local moisture uptake, analogous to the gravimetric assessment of moisture uptake. This signal is normalised as described by Mohorič et al. (2004).

2.2.8. Descriptive models for water uptake during cooking

1D Signal profiles taken perpendicular to the longitudinal axis of the kernel reveal the nature of water ingress – gradual slopes (Gaussian profile) indicate Fickian diffusion and steep slopes indicate high water demand diffusion. A supplementary procedure of monitoring the diffusion process is obtained by computing the sum of the 1D profiles as a function of time. This integrated signal is then normalised according to the moisture content of equilibrated cooked kernels determined by gravimetry. The signal integrated over the volume of the kernel as a function of time gives an estimate of the hydration rate and cooking time. Two processes run simultaneously during cooking: water ingress and gelatinisation. The latter effect manifests itself as a change of NMR spin relaxation time.

Table 1
Overview of the meso- and microstructural parameters for processed rice kernels. Porosity, mean pore and wall sizes were obtained by μ-CT and image analysis. Bulk density and effective particle density (D_{eff}) were measured by gravimetry and flatbed scanning (van Dalen, 2006). Predominant starch forms (N: native (crystalline), G: gelatinised, R: retrograded, A: A-amylose, B: B-amylose, V: V-amylose, V–l: V-amylose–lipid complex) were determined by DSC and XRD.

Type	M	MP	P	PP	W	WP	E	EP
Dominant starch form	N A	N A	R B, V–l	G	R B, V–l	R B, V	G V, V–l	G V–l
Density (bulk)	0.83	0.52	0.89	0.23	0.66	0.30	0.62	0.47
Density (D_{eff})	1.23	0.89	1.32	0.36	1.11	0.55	1.20	0.92
% Pores	0	35	0	63	9.4	54	1.2	33
Mean pore diameter, mm		0.12		0.95	0.66	0.45	0.52	0.43
Wall size, mm		0.09		0.14	0.59	0.10	0.78	0.16

If gelatinisation and water ingress in a specific voxel concur – starch gelatinises as water reaches it – and if the diffusion is well described by Fickian diffusion, then a first-order model describing exponential saturation of moisture content with a characteristic hydration time τ'

$$m = m_0[1 - \exp(-T/\tau')], \quad (2)$$

where T is the time of cooking, can be used to quantify the hydration process.

In the case of the kernel having large interconnected pores, water can penetrate the kernel even without heat and moisture ingress is faster. Here the integrated signal does not monotonically increase as water is taken in, because water inside the kernel is absorbed in the starch with a certain rate during gelatinisation, which changes the signal relaxation time. The signal of a pixel is in this case given by:

$$S = m_w R_w + m_g R_g, \quad (3)$$

where m_w is the mass of bulk water and m_g the mass of water forming the gel. The different phases, free water and gel, contribute with corresponding weights, R_g and R_w, given by transversal relaxation and saturation:

$$R_{w,g} = [1 - \exp(-TR/T_{1w,g})]\exp(-TE/T_{2w,g}). \quad (4)$$

The transverse relaxation time of free water T_{2w} is longer than the transverse relaxation time of gel T_{2g}. If we assume exponential absorption of water in gel with the rate τ then the amount of free water decays as $m_w = m_0\exp(-T/\tau)$, where m_0 is the total amount of water. As water ingresses in the voxel with the rate τ': $m_0 = m[1 - \exp(-T/\tau')]$, the signal is given by

$$S = m[1 + r\exp(-T/\tau)][1 - \exp(-T/\tau')]R_g. \quad (5)$$

Here $r = (R_w - R_g)/R_g$.

Other cases of diffusion and gelatinisation cannot be easily described analytically and numerical simulations based on water demand driven diffusion as described below are more suitable. These simulations are very intensive, and it only makes sense to perform these for the three classes described in the results section.

2.2.9. Structure-based simulation of water uptake during cooking

A model for water uptake in a rice kernel should take into account the different types of diffusion in a substrate and the swelling of the substrate as a result of water uptake. Furthermore, the model should be applicable to homogeneous substrates, i.e. substrates without any pores, as well as to inhomogeneous substrates, i.e. substrates that contain pores or substrates that only consist of a network of thin interconnected walls. Our model (van den Doel et al., in press) represents a substrate on a uniform grid with each grid element or voxel corresponding to a fixed-volume. With a fixed-volume grid, swelling of the substrate implies transport of (moist) the substrate mass among its neighbours. The volume occupied by the mixture mass (substrate and water) can vary from zero, at the positions of the pores, to the maximum volume of a voxel in the case of the presence of substrate and water. These

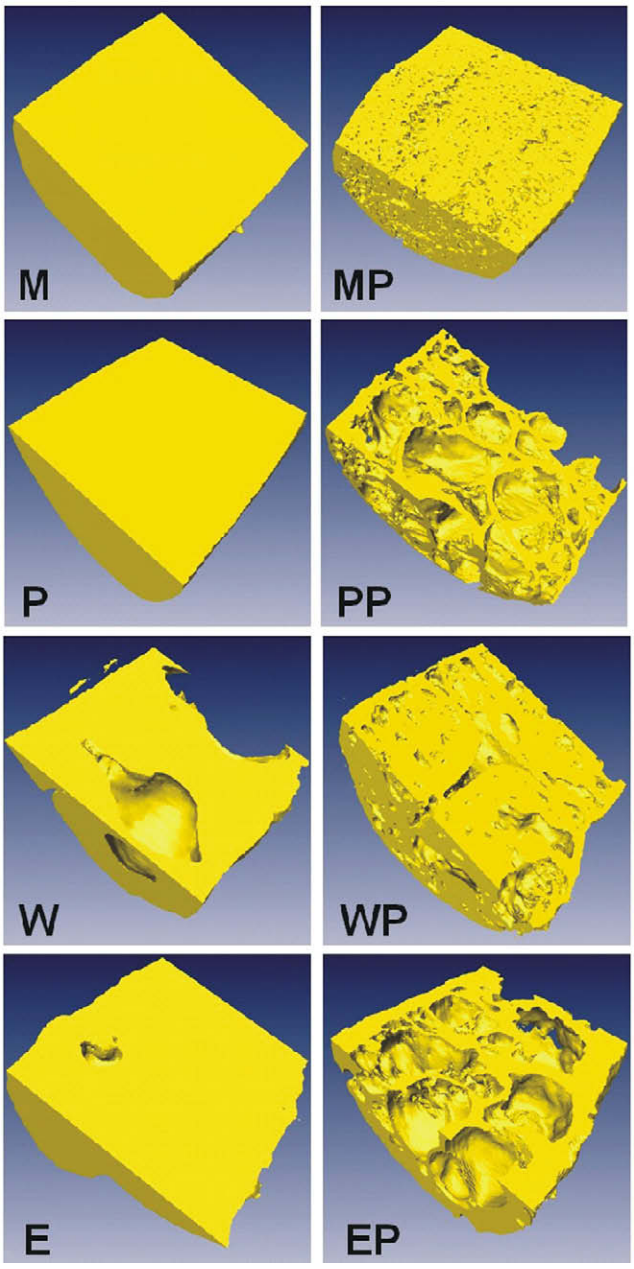

Fig. 1. 3D Reconstruction of the interior of rice kernels imaged by μ-CT (length = 1.8 mm).

differences of occupied volume are described by the saturation level, i.e. the fraction of voxel volume occupied by the mixture of starch and water. If fully saturated the moistured substrate takes up any water, then that water uptake forces some of the moistured substrate out of that voxel into its neighbouring voxels. Completely occupied saturated voxels remain completely occupied and the only increase in water content can be achieved at the expense of starch. In partially occupied voxels the rate of change of the starch distribution is zero as long as the voxel is not completely filled, i.e. water is allowed to penetrate the voxel, but since there is room available for the water, no starch is forced out of the voxel. In the partially occupied case both the increase in water content and the saturation level depend on the water influx. The water flux is not given by the water concentration gradient but rather by the WD gradient. The WD depends on the terminal extent of gelatinisation, which itself is a function of the temperature and is linearly proportional to the water fraction. In our simulations we used the WD functions corresponding to Fickian diffusion (low WD diffusion), high WD diffusion and WD function based on the terminal extent of gelatinisation as described by van den Doel et al. (in press).

4. Results and discussion

3.1. Characterisation of rice kernel mesostructure by DSC and XRD

DSC and XRD were used to characterise the type of starch in the processed rice samples. The dominant starch forms present are listed in Table 1. Milled rice (M) and puffed milled rice (MP) show mainly A-type crystalline starch. The non-puffed pre-gelatinised rice samples (P, W) clearly show the presence of B-type crystalline starch. The amount of B-type in the wet-processed sample W is rather large. V-amylose–lipid complexes are found, to a large extent, in both extruded rice samples (E, EP), to a lower extent in wet-processed rice (W, WP) and to a minor extend in non-puffed parboiled rice (P). The phase transition of V-amylose–lipid complexes observed with DSC at 100 and 115 °C is supported by the

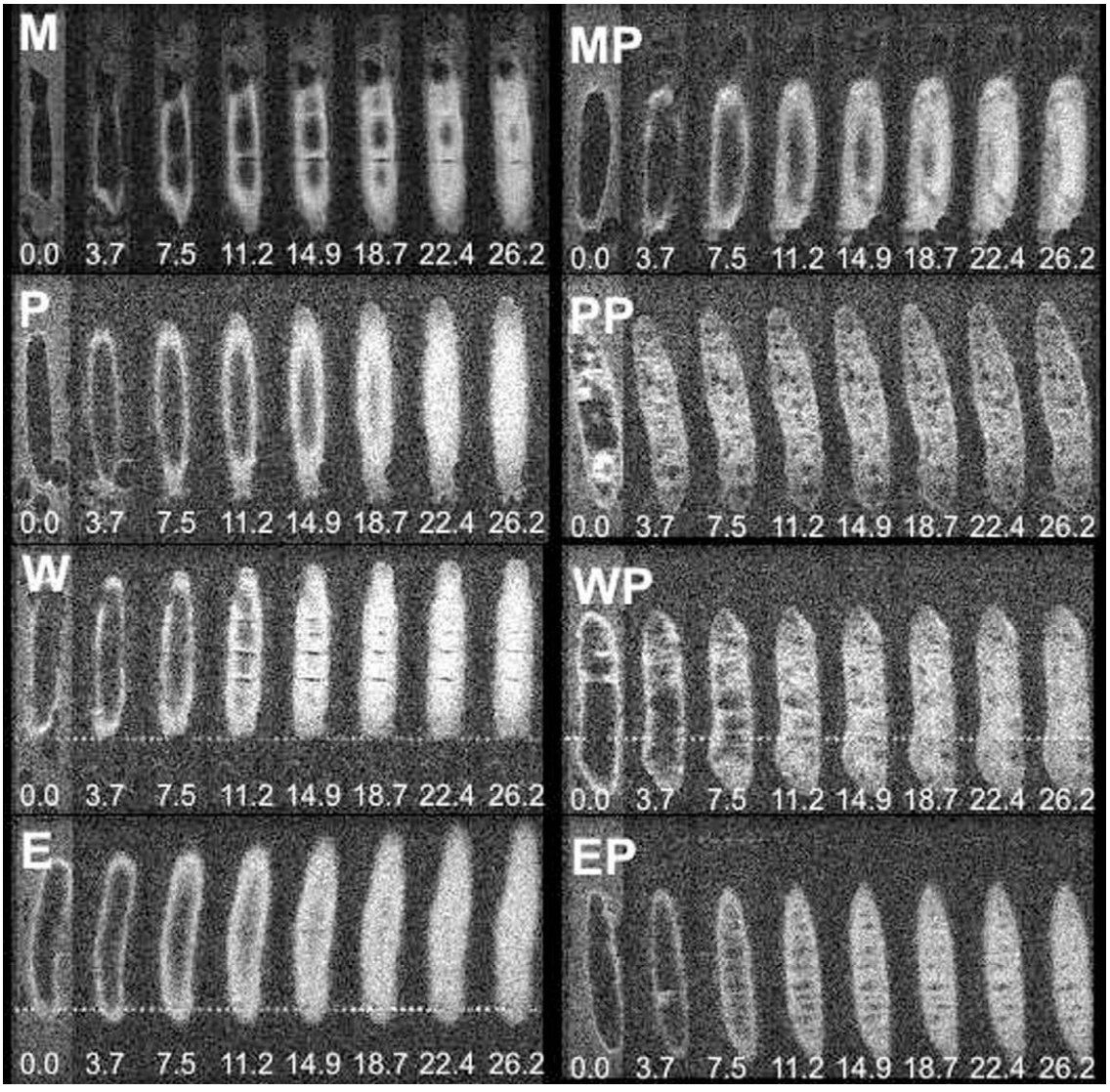

Fig. 2. Series of MRI images through the centre of the kernel representing the cooking process at different times indicated at the bottom in minutes. The left column represents from top to bottom, milled (M), parboiled (P), wet-processed (W), and extruded (E) kernels, respectively. The right column represents milled and puffed (MP), parboiled and puffed (PP), wet-processed and puffed (WP) and extruded and puffed (EP) kernels, respectively. Only every third frame of the total cooking series is shown for brevity.

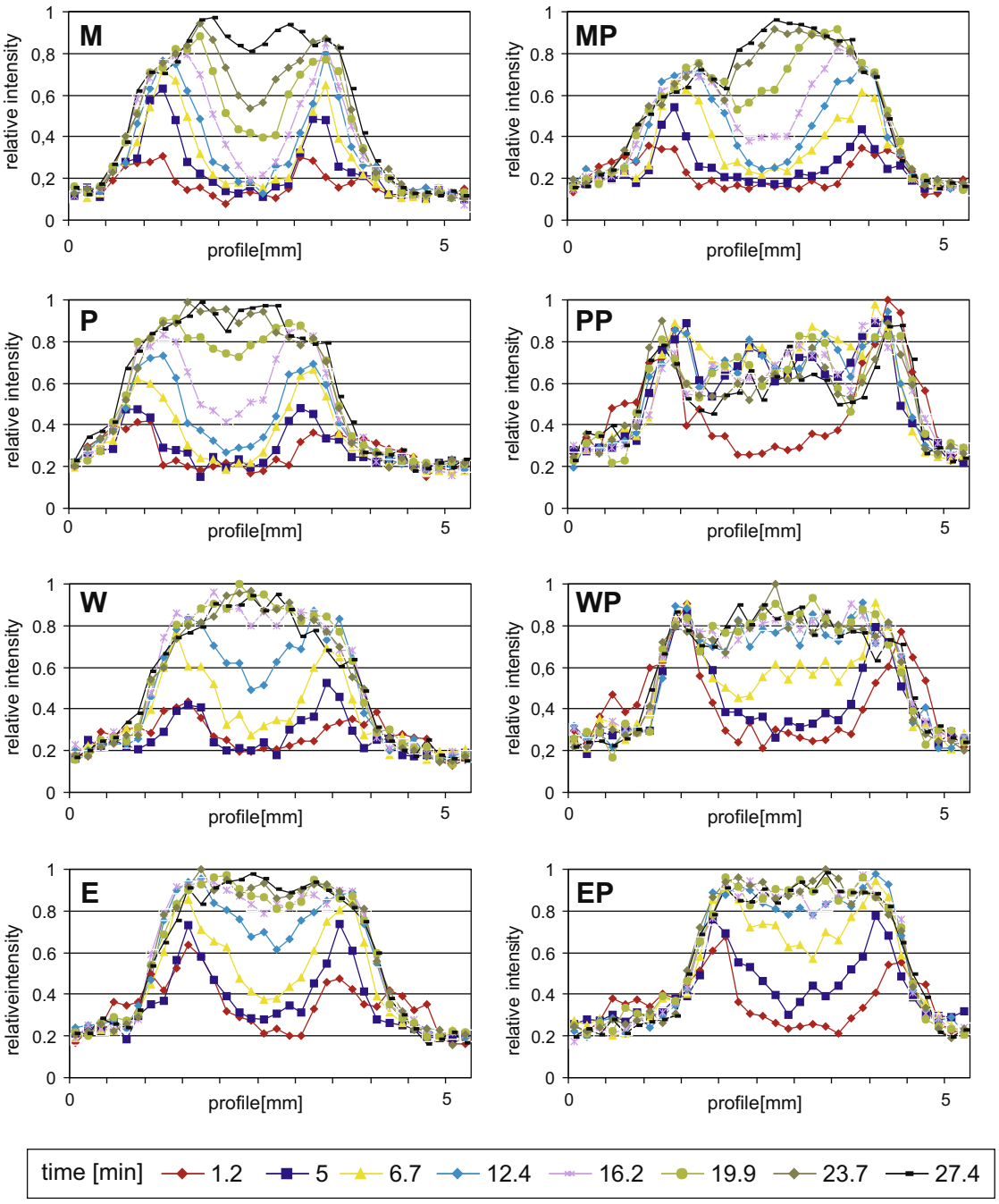

Fig. 3. 1D MRI intensity plots across the centre of the central slice showing the moisture profile of the kernel during cooking. The horizontal axis represents the spatial dimension across the kernel and the vertical axis represents the relative moisture content. Shown are graphs for the different rice types (coding explained in the text and the caption of Fig. 2).

XRD diffraction pattern of V-type starch. It is suggested that the various pregelatinisation procedures induce formation of V-amylose–lipid complexes. The samples (P, W) that show large peaks at 55 °C (recrystallised or retrograded amylopectin) in the DSC thermograms, show large peaks at the B-type crystals positions in the XRD diffractograms. It is suggested that retrograded amylopectine preferentially forms the more open packed B-form.

3.2. Characterisation of rice kernel microstructure by μ-CT

The porous microstructure of the kernels was determined by μ-CT. The contrast in μ-CT images is based on the difference in absorption of X-rays by the constituents of the sample. For the kernels under study this implied that the contrast was dominated by air and the solid matrix. The 3D images of selected parts of all kernel types are shown in Fig. 1. They show the dramatic effect of puffing on the microstructure of the rice kernels. To a lesser extent one can also observe effects of wet-processing (W) and extrusion (E) on kernel porosity. The porous structure of the kernels in terms of pore sizes and wall thickness distribution was obtained from the grey-value μ-CT images, avoiding the need for segmentation. Molecular sieving (Hendriks, van Kempen, & van Vliet, 2007) was applied to the images, which involves morphological filtering at different scales, i.e. grey-value opening for the pore sizes and grey-value closings for the wall sizes. This yields a scalespace, from which a volume-weighted cumulative size distribution can be

Table 2
Description of water uptake classes.

Class 1	Difficult water uptake at the edge, later high WD driven diffusion, pore structure (if present) plays no important role (M, MP)
Class 2	Fickian diffusion (low WD) during complete course of water uptake, pore structure (if present) plays no important role
Class 2A	The uptake of water near the edges is hampered (P, W)
Class 2B	Water is free to enter the kernel (E)
Class 3	Easy water uptake at the edge as well as in the interior of the rice kernels. Pore structure is connected and open to the outside, thus facilitating water uptake (PP, WP, EP)

obtained. By thresholding the μ-CT images, one can also assess the percentage and average size of the pores. The results of pore size and porosity measurements are shown in Table 1. One can assess the effect of the different processing steps on kernel microstructure in a quantitative manner. In the milled (M) and parboiled (P) types no (μ-CT observable) pores are formed. Extrusion (E) produces hardly any porosity (around 1%) and roughly a tenth of the volume of wet-processed kernels (W) consists as pores. The largest porosity and pore sizes are induced in the kernels that are puffed dry from high moisture content, i.e. the PP, WP, MP and EP types. Mean pore diameters range from 0 mm (M, P), 0.1 mm (MP), around 0.5 mm (W, WP, E, EP) to almost 1 mm for PP.

3.3. Spatio-temporal assessment of water uptake by MRI

Fig. 2 shows MRI scans of the rice kernels during cooking as a series of 2D cross-section images of the central slices of the 3D sets of images. The series of images in a single row depict a specific rice type during cooking and images follow in time as indicated by marks (in minutes) at the bottom of each image. Only the protons of water molecules contribute to the pixel intensity in MRI images. The signal from starch itself is negligible, because it's transverse relaxation time is shorter than 1 ms. Water molecules that are incorporated in the crystalline starch cannot be detected by the MRI method and parameters used, but can be observed after gelatinisation, and their concomitant increase in molecular mobility. Sorption isotherm data (van den Berg, 1981) suggest that in starch with a moisture content below 10%, water is very strongly associated with the starch molecules, which explains the short relaxation time.

At the beginning of the series the kernel signal is barely above the noise level and the signal of free water around the kernel emphasises glass beads and tube walls. Only PP and WP kernels show pores filled with water. A stronger signal is also observed in the peripheral layer of the kernel. A possible reason can be water interacting with the kernel surface or a susceptibility effect, leading to a shorter T_1, and thus less T_1 saturation (Scheenen et al., 2000). This layer is possibly equivalent to the layer of gelatinised starch reported in He and Suzuki (1987). The signal of free water around the kernel disappears in the rest of the series because diffusion and convection increase with temperature. As water diffuses into the kernel, the images reveal the internal structure. The structural heterogeneities disappear as the cooking process continues and the starch gelatinises and swells. Clearly visible in the MR images are cracks which develop in milled kernels during storage in a dry compartment. Hydration along the cracks is significantly faster (around 25 min) than in the bulk starch (around 30 min). Pores in processed kernels can be clearly distinguished even at the relatively low resolution. Some pores get hydrated even before the cooking process is initiated. This is possible when pores are connected to the surface and an escape route for the trapped air exists.

3.4. Classification of water uptake during cooking based on descriptive models

In Fig. 3 the uptake of water in the investigated rice kernels is presented as 1D transversal MRI intensity profiles where the moisture fronts are clearly visible. They can be used to evaluate the rate of hydration and the process governing it, namely, Fickian or high WD driven diffusion. One can recognise three classes of water uptake, which are summarised in Table 2. The profiles of M and MP types reveal a relatively slow increase in water content. This implies that water uptake at the boundary of these rice kernels is slow. Furthermore, the profiles in the interior of kernels show steep water fronts moving inwards. This would imply that the

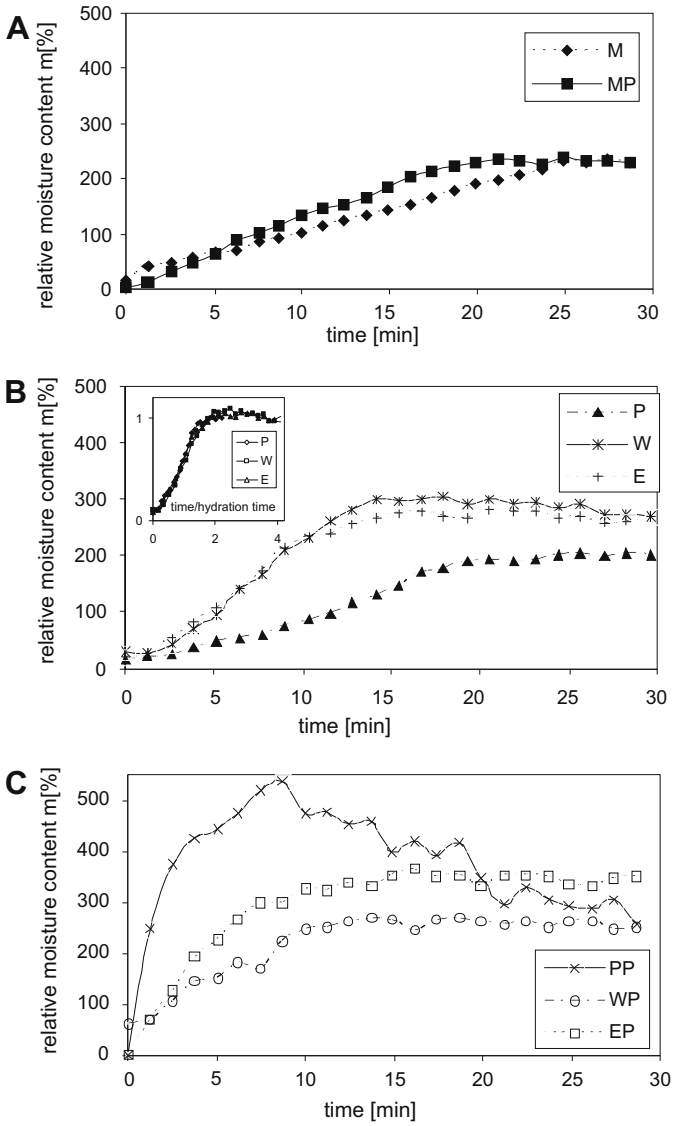

Fig. 4. Increase in relative moisture content in rice kernels during cooking. The relative moisture content is determined from integration of the MRI signal of the kernel and is normalised to the moisture content as determined by gravimetric measurements. In A, B, and C the water uptake graphs are shown for kernels classified as Class 1 (M, MP), Class 2A (P, W), Class 2B (E) and Class 3 (PP, WP, EP), respectively. The insertion in B represents relative moisture content vs. time normalised to hydration time.

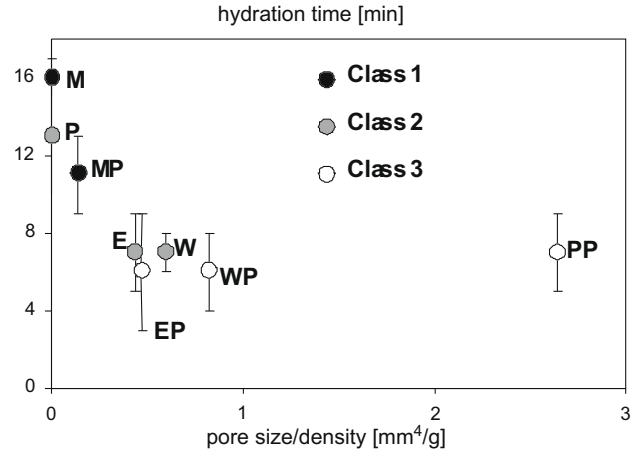

Fig. 5. The relation between the average pore size normalised by kernel density, as determined by μ-CT, and the cooking time as measured by MRI. The different classes are indicated. Class 1 inhibit the types with the smallest pores and the longest hydration times, then follows Class 2 and the Class 3 kernels have the largest pores and the shortest hydration times.

diffusion process is governed initially by Fickian diffusion and later by a high WD driven diffusion. Whereas the milled rice kernel shows isotropic diffusion fronts, these appear anisotropic for the puffed kernel. The anisotropy in diffusion can be attributed to pores that are too small to generate an open structure, as observed for other kernels. M and MP kernels represent Class 1 of water uptake behaviour. P, W and E kernels show Gaussian water uptake profile, which is indicative of Fickian diffusion, and are here designated as Class 2 behaviour. P and W kernels initially take up water slowly, likely because of structures at the boundary of the kernel. Such behaviour is classified as Class 2A uptake. This stands in contrast to the behaviour of E kernel where the water content near the boundary is more or less instantly at the maximum value. This can be explained by the absence of any internal structure in these kernels due to the extrusion processing step. Such kernels are attributed to Class 2B. Rice types PP, WP and EP are puffed and consist of a very open porous structure. This facilitates easy penetration of water into the kernel, before actually being taken up by the starch. This explains the uniform increase of the water content throughout the entire rice kernel. When water uptake in rice kernels is completely determined by the porous structure of the rice kernel we designate this as Class 3 behaviour.

The classification of kernels in Classes 1, 2 and 3 is further illustrated by considering the integrated MRI signal during cooking. Properly normalised (in such manner that maximal NMR signal corresponds to the saturated moisture content as measured by gravimetry) integrated signals in Fig. 3 yield the curves for different rice types as shown in Fig. 4. Different classes can be distinguished by the initial shape of the integrated curve. If the curve starts as a straight line, the type falls into Class 1, the concave and convex shapes represent Classes 2 and 3, respectively. The curves for P or EP type kernels follow the model described by Eq. (1) which corresponds to Fickian diffusion and falls into Class 1 or 3. In contrast the plot for PP type kernels fits to the model described by Eq. (5) and the best fit to the data gives the following values: $\tau = (7.5 \pm 0.3)$ min, $\tau' = (17 \pm 4)$ min and $r = 11 \pm 3$. Although both PP and EP kernels fit into Class 3, they differ with respect to the rate of water absorption in the starch – in EP starch absorbs water with a high enough rate to prevent the two phase effect on the MRI signal. Class 2 represents P, W and E types, whereby type P clearly differs from W and E unless drawn on a master curve, where time is normalised to hydration time (see below) and the moisture content is normalised to final moisture content (see inset in Fig. 4B).

Characteristic hydration times – defined as the time needed to reach $(1 - 1/e)$ the final moisture content – are depicted in Fig. 5. The plot shows the relation between the average pore sizes normalised by average density and the characteristic hydration time for the different rice types. Class 1 types with the smallest pores have

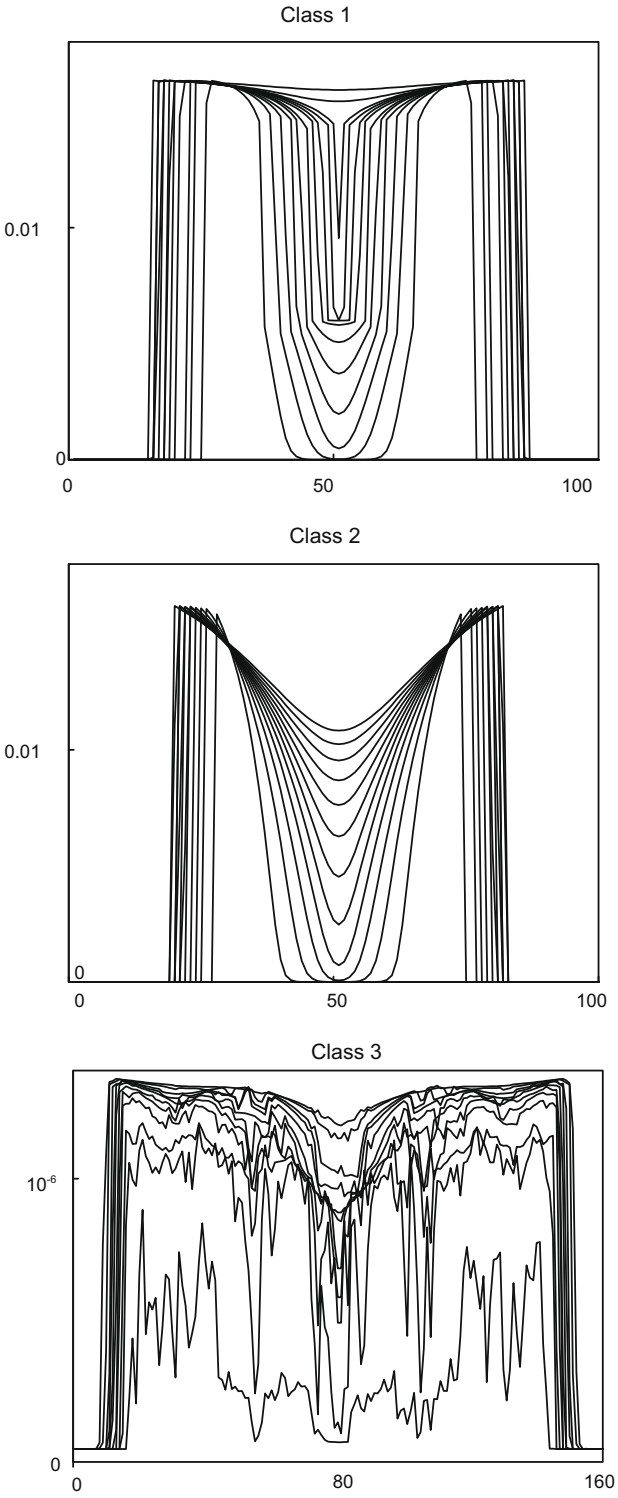

Fig. 6. Simulations of water uptake during cooking in rice kernels classified as Classes 1, 2 and 3. The simulations of Class 1 and Class 2/3 water uptake behaviour, respectively, used a high WD and low WD (Fickian) function. Simulations for Classes 1 and 2 are based on 1D rice kernels. The simulation for Class 3 is based on an actual μ-CT 3D image of a puffed rice kernel (PP) and a low WD (Fickian) function; profiles are averaged over an axial cross-section of the rice kernel.

the longest hydration times, Class 2 follows and the Class 3 kernels have the largest pores and the shortest hydration times.

3.5. Structure-based simulation of water uptake during cooking

Fig. 6 shows the transversal moisture profiles from numerical simulations of Classes 1, 2 and 3 diffusion. The simulations of Classes 1 and 2 are based on solid 1D rice kernels. The simulation of Class 3 is based on a 3D porous rice kernel structure, as obtained by μ-CT. In the simulations, the water content at the boundary is always set to the maximum possible water content. Two different WD functions were tested: a high WD model and a Fickian (low WD) model. In the simulations, we see the steep diffusion fronts for Class 1 diffusion (types M and MP), which is characteristic for high WD driven diffusion. For Class 2 diffusion (types P, W and E), we see the Gaussian profiles which are typical for Fickian diffusion. We note that in these simulations we cannot account for the boundary that is easily or not penetrated by water which would represent Classes 2A and 2B, respectively. The simulated profiles for Class 3 (types PP, WP and EP) result from a 3D porous rice kernel and are averaged over a longitudinal slice. These profiles show a more or less uniform increase of water content which is related to the very open structure of these rice kernels, in which water immediately penetrates the complete pore structure, where it can be taken up by the starch.

4. Conclusion

A novel MRI method allows observation of the ingress of water in rice kernels during cooking in real-time mode, and with good spatial resolution in 3D. Descriptive modelling of the MRI data reveals three main classes (Classes 1–3) of cooking behaviour. In Class 1 relatively steep fronts are observed and outer layers are hydrated before the front ingresses. In Class 2 Gaussian profiles can be distinguished and the core of the kernel hydrates almost uniformly. The swelling of the kernel is negligible, since pores themselves provide ample space into which the substrate can expand. Fronts are sharp in this case as well. Class 3 behaviour is typical for a very open porous structure. This facilitates easy penetration of the water in the kernel, before actually being taken up by the starch, explaining the uniform increase of the water content throughout the entire rice kernel. These MRI observations match with simulations based on a structure-based model that comprised the concept of Water Demand as well as microstructural heterogeneity (e.g. pores and cracks) as determined by μ-CT. We can conclude that increasing the porosity of rice kernels generally reduces the cooking time but only to a certain extent. Another contributing factor is the mesostructural order of starch; in the processed rice the native granular structure is associated with slow high WD driven diffusion, whereas in retrograded and amorphous starch one observes faster Fickian (low WD) type diffusion.

Acknowledgements

The authors would like to thank various colleagues at Unilever R&D Vlaardingen for their help and advice in this work. This work received funding from the Dutch BTS Program (Dutch Ministry of Economical affairs) as Project BTS00103.

References

Bhattacharya, K. R. (1985). Parboiling of rice. In B. O. Juliano (Ed.), *Rice chemistry and technology* (pp. 289–348). St Paul Minnesota, USA: American Association of Cereal Chemists.

Blakeney, A. B. (1996). Rice. In R. J. Henry & P. S. Kettlewell (Eds.), *Cereal grain quality* (pp. 55–76). London: Chapman and Hall.

Chandrasekhar, P. R., & Chattopadhyay, P. K. (1990). Studies on microstructural changes of parboiled and puffed rice. *Journal of Food Processing and Preservation, 14*(1), 27–37.

Fukuoka, M., Mihori, T., & Watanabe, H. (2000). MRI observation and mathematical model simulation of water migration in wheat flour dough during boiling. *Journal of Food Science, 65*, 1343–1348.

Guha, M. (2006). Extrusion cooking of rice: Effect of amylose content and barrel temperature on product profile. *Journal of Food Processing and Preservation, 30*(6), 706–716.

Gomi, Y., Fukuoka, M., Mihori, T., & Watanabe, H. (1998). The rate of starch gelatinization as observed by PFG-NMR measurement of water diffusivity in rice starch/water mixtures. *Journal of Food Engineering, 36*, 359–369.

Gonzalez, R. J., Torres, R. L., De Greef, D. M., & Guadalupe, B. A. (2006). Effects of extrusion conditions and structural characteristics on melt viscosity of starchy materials. *Journal of Food Engineering, 74*(1), 96–107.

He, G. C., & Suzuki, H. (1987). The relationship between translucency of rice grain and gelatinization of starch in the grain during cooking. *Journal of Nutritional Science and Vitaminology, 33*, 263–273.

Hendriks, C. L. L., van Kempen, G. M. P., & van Vliet, L. J. (2007). Improving the accuracy of isotropic granulometries. *Pattern Recognition Letters, 28*(7), 865–872.

Horigane, A. K., Engelaar, W. M. H. G., Toyoshima, H., Ono, H., Sakai, M., Okubo, A., et al. (2000). Differences in hollow volumes in cooked rice grains with various amylose contents as determined by NMR microimaging. *Journal of Food Science, 65*(3), 408–412.

Kasai, M., Lewis, A., Ayabe, S., Hatae, K., & Fyfe, C. A. (2007). Quantitative NMR imaging study of the cooking of Japonica and Indica rice. *Food Research International, 40*, 1020–1029.

Kasai, M., Lewis, A., Marica, F., Ayabe, S., Hatae, K., & Fyfe, C. A. (2005). NMR imaging investigation of rice cooking. *Food Research International, 38*, 403–410.

Lai, H. M., & Cheng, H. H. (2004). Properties of pregelatinized rice flour made by hot air or gum puffing. *International Journal of Food Science and Technology, 39*(2), 201–212.

Lee, E. Y., Lim, K. I., Jae-Kag, L., & Seung-Taik, L. (2000). Effects of gelatinisation and moisture content of extruded starch pellets on morphology and physical properties of microwave-expanded products. *Cereal Chemistry, 77*, 769–773.

Mariotti, M., Alamprese, C., Pagani, M. A., & Lucisano, M. (2006). Effect of puffing on ultrastructure and physical characteristics of cereal grains and flours. *Journal of Cereal Science, 43*, 47–56.

Mohorič, A., Vergeldt, F., Gerkema, E., de Jager, A., van Duynhoven, J., van Dalen, G., et al. (2004). Magnetic resonance imaging of single rice kernels during cooking. *Journal of Magnetic Resonance, 171*, 157–162.

Murugesan, G., & Bhattacharya, K. R. (1986). Studies on puffed rice. 1. Effect of processing conditions. *Journal of Food Science and Technology – Mysore, 23*(4), 197–202.

Ramesh, M., Bhattacharya, K. R., & Mitchell, J. R. (2000). Developments in understanding the basis of cooked-rice texture. *Critical Reviews in Food Science and Nutrition, 40*(6), 449–460.

Ruan, R. R., Zou, C., Wadhawan, C., Martinez, B., Chen, P. L., & Addis, P. (1997). Studies of hardness and water mobility of cooked wild rice using NMR. *Journal of Food Processing and Preservation, 21*, 91–104.

Scheenen, T. W. J., van Dusschoten, D., de Jager, P. A., & Van As, H. (2000). Microscopic displacement imaging with pulsed field gradient turbo spin-echo NMR. *Journal of Magnetic Resonance, 142*, 207–215.

Stapley, A. G. F., Hyde, T. M., Gladden, L. F., & Fryer, P. J. (1997). NMR imaging of the wheat grain cooking process. *International Journal of Food Science and Technology, 32*, 355–375.

Takeuchi, S., Fukuoka, M., Gomi, Y., Maeda, M., & Watanabe, H. (1997). An application of MRI to the real time measurement of the change of moisture profile in a rice grain during boiling. *Journal of Food Engineering, 33*, 181–197.

Takeuchi, S., Maeda, M., Gomi, Y., Fukuoka, M., & Watanabe, H. (1997). The change in moisture distribution in a rice grain during boiling as observed by NMR imaging. *Journal of Food Engineering, 33*, 281–297.

van Dalen, G. (2006). Characterisation of rice using flatbed scanning and image analysis. In A. P. Riley (Ed.), *Food policy, control and research* (pp. 149–186). New York: Nova Biomedical.

van Dalen, G., Nootenboom, P., van Vliet, L. J., Voortman, L., & Esveld, E. (2007). 3D Imaging, analysis and modelling of porous cereal products using X-ray microtomography. *Image Analysis and Stereology, 26*, 169–177.

van den Berg, C. (1981). *Vapour sorption equilibria and other water starch interactions: A physico chemical approach*. Ph.D. Thesis. Wageningen; Agricultural University.

van den Doel, L. R., Mohoric, A., Vergeldt, F., van Duynhoven, J., Blonk, H., Van As, H., et al. (in press). Mathematical modelling of water uptake through diffusion in 3D swelling substrates. *AiChE Journal*.

Watanabe, H., Fukuoka, M., Tomiya, A., & Mihori, T. (2001). A new non-Fickian diffusion model for water migration in starch food during cooking. *Journal of Food Engineering, 49*, 1–6.